

# Application of Graph Theory in Stability Analysis of Meshed Microgrids

Shivkumar V. Iyer, Madhu N. Belur and Mukul C. Chandorkar, *Member, IEEE*

**Abstract**—This paper studies microgrids where loads are supplied by parallel connected inverters controlled by decentralized active power/voltage frequency and reactive power/voltage magnitude droop control laws. The implementation of droop control laws for sharing of power between inverters has been known to present stability problems particularly for large values of active power/voltage frequency droop control gains. Stability analysis of the microgrid requires a mathematical formulation of the interaction between the inverters due to their droop control laws. However, a simple and elegant mathematical model resulting in a conclusive proof of stability has been found to be lacking in reported literature. In this paper, a state dynamical model has been derived by combining active power flow equations with the active power/voltage frequency droop control laws. Using an analogy between the model matrix and connected graphs, a proof of stability of the microgrid has been stated as a theorem. The paper further examines the limitations of the proof and the difference between the results of the proof and reported practical results.

**Index Terms**—Microgrids, inverters, decentralized control, droop control laws, connected graphs.

## I. INTRODUCTION

Stability analysis in the context of high voltage bulk power transmission systems is well established. Determination of stable boundaries of power systems is achieved using the swing equations of generators and the equal area criterion. A multi-generator power system loses stability when the generators lose synchronism due to faults in the system or excessive variation in the active power demanded by loads. Computational techniques have been developed to analyze the stability of large power systems and are used by practicing engineers.

In this paper, the microgrid will be formed of inverters that are controlled in a decentralized manner by droop control laws. The droop control laws make the inverters emulate synchronous generators by varying the frequency and magnitude of the output voltage of the inverters with respect to the power supplied by the inverter [1]. The  $p$ - $\omega$  droop control law varies the frequency  $\omega$  with respect to the active power  $p$  supplied by the inverter while the  $q$ - $V$  droop control law varies the magnitude  $V$  with respect to the reactive power  $q$  supplied [1]. With the inverters being controlled in a decentralized manner without any communication between them, it becomes essential to examine the stability of the microgrid due to the interaction between the inverters and the effect of the droop controllers.

Shivkumar V. Iyer, Madhu N. Belur and Mukul C. Chandorkar are with the Department of Electrical Engineering of Indian Institute of Technology Bombay, INDIA. Their e-mail IDs are {shivkvi, belur, mukul}@ee.iitb.ac.in.

These autonomous inverter-based microgrids are a relatively new concept. With microgrids gaining popularity, the size and complexity of microgrids are bound to increase. Therefore, there arises a need to develop techniques of stability analysis for microgrids. Microgrids differ from bulk power systems in a few significant aspects. The inverters in the microgrids are inertia-less as opposed to the generators in bulk power systems and therefore swing equations for inverters are not applicable. The inverters do not have substantial overload capacities unlike synchronous generators and therefore transient studies are extremely important to determine the peak currents that the inverters will have to supply. Microgrids at the distribution level voltage have cables that possess high R/X ratio as compared to the negligible R/X ratio of transmission lines in bulk power systems. The above listed differences make stability analysis in microgrids a challenging topic of research.

With the inverters being controlled using inputs as active power  $p$  and reactive power  $q$  supplied by them, a mathematical model can be derived using equations of power flowing between the inverters. Such a mathematical model was proposed by Chandorkar et al [1] where the stability of the microgrid with respect to the  $p$ - $\omega$  droop control laws were examined. The microgrid was represented mathematically by a state dynamical equation with the state variables being the phase angle differences between the output voltages of the inverters in the microgrid. The mathematical model proved the stability of the microgrid with respect to the  $p$ - $\omega$  droop control laws for ring and radial microgrids.

In this paper, the mathematical model has been extended to meshed microgrids with arbitrary connections as most practical microgrids will contain complex interconnections. Moreover, the proof of stability of the microgrid will be performed using concepts from graph theory and will be stated as a theorem. The differences between the stability result obtained analytically and those obtained from practical results will be compared and the reasons for these differences will be examined.

The outline of the paper is as follows. Section 2 derives the mathematical model of the microgrid using active power flow equations and  $p$ - $\omega$  droop control laws. Section 3 introduces concepts of graph theory and presents a proof of stability of the microgrid. Section 4 describes the limitation of the mathematical model in its inability to provide the stable boundaries of the microgrid accurately.

## II. MATHEMATICAL MODEL DERIVATION

In this section, the topology of the microgrid used for deriving the mathematical model will be described. The model

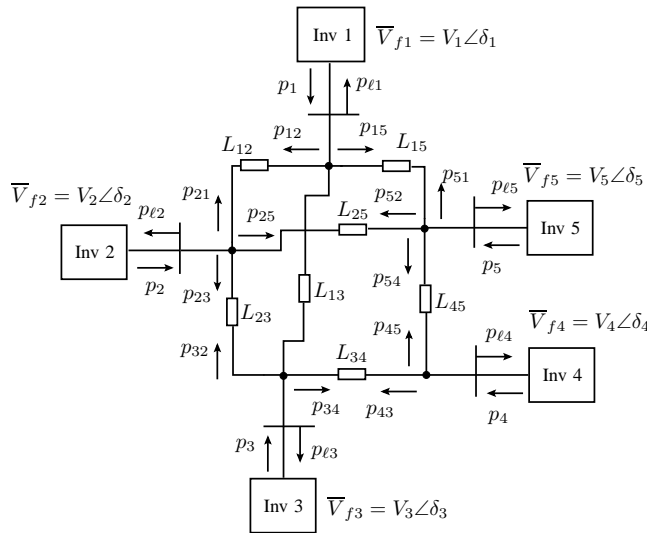


Fig. 1. Microgrid Topology

will be generalized to make it applicable to any arbitrary microgrid. Fig. 1 is a single line diagram showing the topology of a three phase five inverter meshed microgrid. Each of the blocks represented by “Inv” stand for three phase inverters.  $L_{12}, L_{23}, L_{34}, L_{45}, L_{13}, L_{15}, L_{25}$  are the inductances of the interconnecting cables between the inverters with the resistances of the cables being neglected. Fig. 1 also shows the power flowing in the interconnecting cables between the inverters. In Fig. 1, only the active power flows are shown since this paper deals with only the  $p$ - $\omega$  droop control laws. The terminology used for the power flowing between inverters is described taking the interconnection between Inverter 1 and Inverter 2 as an example.  $p_{12}$  is the active power flowing from Inverter 1 to Inverter 2 through the cable connecting them.  $p_1, p_2, p_3, p_4$  and  $p_5$  are the active powers supplied by the inverters.  $p_{\ell 1}, p_{\ell 2}, p_{\ell 3}, p_{\ell 4}$  and  $p_{\ell 5}$  are the active power demanded by the loads connected locally to the five inverters.

The following assumptions will be made that simplify the derivation of the mathematical model:

- 1) The internal dynamics of the inverters are very fast as compared to the dynamics of the interaction between the inverters due to the droop control laws. Therefore, the inverters are assumed to be ideal voltage sources whose output voltages are determined by the references generated by the droop control laws.
- 2) The inverters are further assumed to be controlled power sources that have the capacity to change their power output as desired. This assumption is an essential requirement in the mathematical formulation using power balance laws.
- 3) The loads in the microgrid are assumed to draw a total three phase active and reactive power that has a constant value. This is the case with loads that are balanced linear passive loads.
- 4) This paper will focus on the  $p$ - $\omega$  droop control laws since these are known to have a strong impact on the stability of the microgrid. The magnitudes of the inverter output voltages will be considered constant as the  $q$ - $V$

droop control laws are neglected.

From Fig. 1, the following active power balance equations are written

$$\begin{aligned}
 p_1 &= p_{12} + p_{13} + p_{15} + p_{\ell 1}, \\
 p_2 &= p_{21} + p_{23} + p_{25} + p_{\ell 2}, \\
 p_3 &= p_{31} + p_{32} + p_{34} + p_{\ell 3}, \\
 p_4 &= p_{43} + p_{45} + p_{\ell 4}, \\
 p_5 &= p_{51} + p_{52} + p_{54} + p_{\ell 5}.
 \end{aligned} \tag{1}$$

It is to be noted that the assumption of balanced three phase three wire system is important. In such a balanced three phase system, the power flows marked in Fig. 1 will be constant values. However, if the system is unbalanced due to inequality of the line resistances or inductances in the three phases or due to the connection of unbalanced or non-linear load, the power flows will not be constant values.

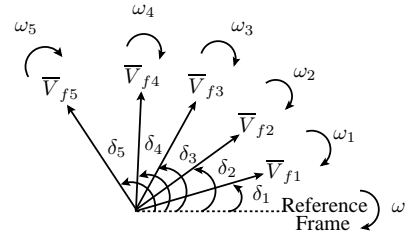


Fig. 2. Inverter output voltage vectors

Fig. 2 shows a sample case of output voltage vectors of the inverters as complex quantities in polar form. The exact placement of the voltage vectors will depend on the loading conditions at the inverters and the  $p$ - $\omega$  droop control gains of the inverters. The output voltages of the inverters shown are  $\bar{V}_{f1} = V_1\angle\delta_1, \bar{V}_{f2} = V_2\angle\delta_2, \bar{V}_{f3} = V_3\angle\delta_3, \bar{V}_{f4} = V_4\angle\delta_4, \bar{V}_{f5} = V_5\angle\delta_5$ . The magnitudes  $V_1, V_2, V_3, V_4, V_5$  are assumed to be the Root-Mean-Squared (R.M.S) values of the line-to-neutral output voltages. The angles  $\delta_1, \delta_2, \delta_3, \delta_4, \delta_5$  are measured with respect to an arbitrary reference frame and in the figure are shown in an arbitrary manner. Moreover, the vectors are shown widely for clarity though the phase angle differences between the vectors is very small due to small cable impedances in the microgrid. The voltage vectors  $\bar{V}_{f1}, \bar{V}_{f2}, \bar{V}_{f3}, \bar{V}_{f4}, \bar{V}_{f5}$  are rotating with angular frequencies of  $\omega_1, \omega_2, \omega_3, \omega_4, \omega_5$  respectively. The reference frame is rotating with an angular frequency of  $\omega$ . However, at steady state  $\omega_1 = \omega_2 = \omega_3 = \omega_4 = \omega_5 = \omega$ , i.e all the vectors and the reference frame are rotating with the same angular frequency. This vector diagram will be used to compute the power flows between the inverters as will be discussed soon.

Fig. 1 shows the active power flows between the inverters. The active power flowing in the interconnecting cable between Inverter  $m$  and Inverter  $n$  is

$$p_{mn} = \frac{3V_m(V_m - V_n \cos \delta_{mn})R_{mn}}{R_{mn}^2 + (\omega L_{mn})^2} + \frac{3V_m V_n \omega L_{mn} \sin \delta_{mn}}{R_{mn}^2 + (\omega L_{mn})^2} \tag{2}$$

where  $\delta_{mn} = \delta_m - \delta_n$ . As can be seen from (2), the active power flowing in the interconnecting cable between any two inverters  $m$  and  $n$  is dependent on the magnitude of

output voltages  $V_m$ ,  $V_n$  of the inverters and the phase angle difference  $\delta_{mn} = \delta_m - \delta_n$  between the inverters. Assuming, the resistances of the interconnecting cable to be negligible, the active power flow  $p_{mn}$  can be approximated to

$$p_{mn} \approx \frac{3V_m V_n}{\omega L_{mn}} \sin \delta_{mn} \quad (3)$$

The  $p$ - $\omega$  droop control law for Inverter  $m$  is written as

$$\omega_m = \omega_0 - k_{pm} p_m \quad (4)$$

where  $\omega_0$  is the nominal frequency of the microgrid,  $\omega_m$  is the frequency of Inverter  $m$ ,  $p_m$  is the active power supplied by Inverter  $m$  and  $k_{pm}$  is the  $p$ - $\omega$  droop control gain of Inverter  $m$ . The strong coupling between the phase angle difference and the active power flow will decrease if R/X ratio of the cables is considered as is evident from (2). The effect of R/X ratio of the cables will be considered at a later section after the basic proof has been completed.

Equation (3) shows that active power  $p_{mn}$  flowing between Inverter  $m$  and Inverter  $n$  is a nonlinear function of the phase angle difference  $\delta_{mn}$  between the inverter output voltages. Therefore, in order to develop a mathematical model using droop control laws and power flow equations, the equations are linearized about an equilibrium point and the variables are expressed in the small signal domain. The variables are expressed as small deviations about the equilibrium point. For example, variable  $\delta_{mn}$  is replaced by  $\delta_{mn} + \Delta\delta_{mn}$  with  $\delta_{mn}$  being the value of the phase angle difference at the equilibrium point and  $\Delta\delta_{mn}$  is the deviation of the phase angle difference from its value at the equilibrium point. Similarly, variable  $p_{mn}$  is replaced by  $p_{mn} + \Delta p_{mn}$ , variable  $\omega_m$  by  $\omega_m + \Delta\omega_m$ . The inverter output voltage magnitudes  $V_m$  and  $V_n$  are assumed to be constant at this point since the  $q$ - $V$  droop control laws are neglected. The  $p$ - $\omega$  droop controller can be written in the small signal sense as

$$\Delta\omega_m = -k_{pm} \Delta p_m \quad (5)$$

The deviation in the angular frequency  $\Delta\omega_m$  can be written in terms of the deviation in the phase angle as

$$\Delta\omega_m = \frac{d}{dt}(\Delta\delta_m) \quad (6)$$

The power balance laws of (1) can be linearized and expressed in the small signal sense as follows

$$\begin{aligned} \Delta p_1 &= \Delta p_{12} + \Delta p_{13} + \Delta p_{15} + \Delta p_{\ell 1} \\ \Delta p_2 &= \Delta p_{21} + \Delta p_{23} + \Delta p_{25} + \Delta p_{\ell 2} \\ \Delta p_3 &= \Delta p_{31} + \Delta p_{32} + \Delta p_{34} + \Delta p_{\ell 3} \\ \Delta p_4 &= \Delta p_{43} + \Delta p_{45} + \Delta p_{\ell 4} \\ \Delta p_5 &= \Delta p_{51} + \Delta p_{52} + \Delta p_{54} + \Delta p_{\ell 5} \end{aligned} \quad (7)$$

The deviation in the active power flowing between Inverter  $m$  and Inverter  $n$  can be derived from (2) as

$$\begin{aligned} \Delta p_{mn} &= \frac{3V_m V_n \cos \delta_{mn}}{\omega L_{mn}} \Delta\delta_{mn} \\ &= c_{mn} \Delta\delta_{mn} \end{aligned} \quad (8)$$

where

$$c_{mn} = \frac{3V_m V_n \cos \delta_{mn}}{\omega L_{ij}} \quad (9)$$

From the above expression for  $c_{mn}$ , it is evident that  $c_{nm} = c_{mn}$ . Therefore, from (8),  $\Delta p_{nm} = c_{nm} \Delta\delta_{nm} = c_{mn} \Delta\delta_{nm}$ . This relation can also be explained with respect to power balance laws since there is no power loss in the interconnecting cables with their resistances being neglected.

Combining (5), (6), (7), (8) the following matrix equation can be written

$$\frac{d}{dt} \Delta\delta = \mathbf{A}_{kp} (-\mathbf{A}_p \Delta\delta + \Delta\mathbf{p}_L) \quad (10)$$

where

$$\Delta\delta = (\Delta\delta_1, \Delta\delta_2, \Delta\delta_3, \Delta\delta_4, \Delta\delta_5)$$

$$\mathbf{A}_{kp} = \text{diag}(k_{p1}, k_{p2}, k_{p3}, k_{p4}, k_{p5})$$

$$\Delta\mathbf{p}_L = (\Delta p_{\ell 1}, \Delta p_{\ell 2}, \Delta p_{\ell 3}, \Delta p_{\ell 4}, \Delta p_{\ell 5})$$

$$\mathbf{A}_p =$$

$$\begin{bmatrix} c_{12}+c_{13}+c_{15} & -c_{12} & -c_{13} & 0 & -c_{15} \\ -c_{12} & c_{12}+c_{23}+c_{25} & -c_{23} & 0 & -c_{25} \\ -c_{13} & -c_{23} & c_{13}+c_{23}+c_{34} & -c_{34} & 0 \\ 0 & 0 & -c_{34} & c_{34}+c_{45} & -c_{45} \\ -c_{15} & -c_{25} & 0 & -c_{45} & c_{15}+c_{25}+c_{45} \end{bmatrix} \quad (11)$$

where ‘‘diag’’ implies a diagonal matrix with the specified vector along the diagonal of the matrix. The above state dynamical equation has been derived for the microgrid of Fig. 1. However, the derivation of the mathematical model can be generalized for any arbitrary microgrid as follows.

For any general microgrid with a large number of inverters and complex interconnections between the inverters, the following observations can be made. The deviation in the power supplied by a Inverter  $m$  is written as

$$\Delta p_m = \sum_{\{n\}} \Delta p_{mn} + \Delta p_{\ell m} \quad (12)$$

where  $\{n\}$  is the set of inverters which are connected to Inverter  $m$  excluding Inverter  $m$ . The above equation can be simplified to

$$\Delta p_m = \left( \sum_{\{n\}} c_{mn} \right) \Delta\delta_m - \sum_{\{n\}} c_{mn} \Delta\delta_n + \Delta p_{\ell m} \quad (13)$$

Since,  $\frac{d}{dt}(\Delta\delta_m) = -k_{pm} \Delta p_m$  constitutes a row of the representation similar to (10), it can be observed from (13) that the sum of elements along each row of the matrix  $\mathbf{A}_p$  will be zero. The matrix  $\mathbf{A}_p$  will have for element  $mn$ , the term  $-c_{mn}$  if Inverter  $m$  and Inverter  $n$  are connected. If Inverter  $m$  and Inverter  $n$  are not connected, the element  $mn$  of  $\mathbf{A}_p$  will be 0. Since,  $c_{mn} = c_{nm}$ , the matrix  $\mathbf{A}_p$  will be symmetric. Therefore, the sum of elements along each column of  $\mathbf{A}_p$  will also be zero. This special property of the matrix  $\mathbf{A}_p$  is utilized in proving the stability of the microgrid as will be described in the next section.

### III. STABILITY PROOF USING CONCEPTS FROM GRAPH THEORY

A graph is defined as a mathematical structure used to model pairwise relations between objects from a certain collection. The objects are represented by nodes while the interaction between objects is represented by a branch. Fig. 3 shows an example of a graph consisting of five nodes (objects) numbered

from one to five interacting through weighted branches. The interaction between objects  $m$  and  $n$  has weight  $a_{mn}$ . Since the graph is undirected,  $a_{mn} = a_{nm}$ . This section will describe how a graph is used to depict the microgrid with its power flows.

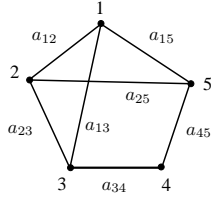


Fig. 3. A connected graph depicting system interaction

For the connected graph of Fig. 3, the following definitions will be provided and details can be found in [2]. The adjacency matrix of the graph is

$$\mathbf{A} = \begin{bmatrix} 0 & a_{12} & a_{13} & 0 & a_{15} \\ a_{12} & 0 & a_{23} & 0 & a_{25} \\ a_{13} & a_{23} & 0 & a_{34} & 0 \\ 0 & 0 & a_{34} & 0 & a_{45} \\ a_{15} & a_{25} & 0 & a_{45} & 0 \end{bmatrix} \quad (14)$$

Because the graph is undirected, the adjacency matrix is symmetric *i.e.*  $\mathbf{A} = \mathbf{A}^T$ . A matrix  $\mathbf{D}$  will be defined such that  $\mathbf{D}$  is a diagonal matrix and the diagonal elements of  $\mathbf{D}$  are the sum of all the elements of  $\mathbf{A}$  in that row.

$$d_{mm} = \sum_{\substack{n=1 \\ n \neq m}}^5 a_{mn} \quad (15)$$

The Laplacian of the connected graph of Fig. 3 is defined as  $\mathbf{L} =: \mathbf{D} - \mathbf{A}$ .

$\mathbf{L} =$

$$\begin{bmatrix} a_{12}+a_{13}+a_{15} & -a_{12} & -a_{13} & 0 & -a_{15} \\ -a_{12} & a_{12}+a_{23}+a_{25} & -a_{23} & 0 & -a_{25} \\ -a_{13} & -a_{23} & a_{13}+a_{23}+a_{34} & a_{34} & 0 \\ 0 & 0 & -a_{34} & a_{34}+a_{45} & -a_{45} \\ -a_{15} & -a_{25} & 0 & -a_{45} & a_{15}+a_{25}+a_{45} \end{bmatrix} \quad (16)$$

The Laplacian  $\mathbf{L}$  is also symmetric. Furthermore,  $\mathbf{L}$  has the property that the number of eigenvalues equal to zero is equal to the number of disjoint parts of the graph. In case of the graph of Fig. 3, there is a single eigenvalue equal to zero. The remaining eigenvalues of  $\mathbf{L}$  are real and positive and  $\mathbf{L}$  satisfies  $\mathbf{L} \geq 0$  [2]. On comparing (16) with the matrix  $\mathbf{A}_p$  of (11),  $\mathbf{A}_p$  can also be interpreted as the Laplacian of a connected graph. The following proof will describe how the property of the Laplacian is used to prove the stability of the microgrid with respect to the  $p$ - $\omega$  droop control law.

*Theorem 1:* The mathematical model of the microgrid with respect to  $p$ - $\omega$  droop control laws is expressed in the form of (10). This representation results in a stable controlled system due to the property of the matrix  $\mathbf{A}_{kp}\mathbf{A}_p$  having real and non-negative eigenvalues. Furthermore, the non-zero eigenvalues of  $\mathbf{A}_{kp}\mathbf{A}_p$  will tend to  $+\infty$  as the control gains in  $\mathbf{A}_{kp}$  tend to  $+\infty$ .

*Proof:* The mathematical model of the microgrid with respect to droop control laws are presented in (10). The discussion above has provided a comparison of (10) for Fig. 1 and (16) for Fig. 3. The matrix  $\mathbf{A}_p$  of (10) therefore is equal

to the Laplacian of the graph of the microgrid. The matrix  $\mathbf{A}_p$  therefore has an eigenvalue equal to zero and the remaining non-zero eigenvalues are real and positive. The eigenvalues of  $\mathbf{A}_{kp}\mathbf{A}_p$  will be determined as follows.

The eigenvalues of  $\mathbf{A}_{kp}\mathbf{A}_p$  are obtained as follows

$$\text{roots}[\det(\lambda\mathbf{I} - \mathbf{A}_{kp}\mathbf{A}_p)] \quad (17)$$

The above equation can be rewritten as

$$\begin{aligned} & \text{roots}[\det(\lambda\mathbf{A}_{kp}^{1/2}\mathbf{A}_{kp}^{-1/2} - \mathbf{A}_{kp}\mathbf{A}_p)] = \\ & \text{roots}[\det(\mathbf{A}_{kp}^{1/2})\det(\lambda\mathbf{I} - \mathbf{A}_{kp}^{1/2}\mathbf{A}_p\mathbf{A}_{kp}^{1/2})\det(\mathbf{A}_{kp}^{-1/2})] \end{aligned} \quad (18)$$

For non-negative droop control gains in  $\mathbf{A}_{kp}$ , the eigenvalues are obtained from

$$\text{roots}[\det(\lambda\mathbf{I} - \mathbf{A}_{kp}^{1/2}\mathbf{A}_p\mathbf{A}_{kp}^{1/2})] \quad (19)$$

The eigenvalues of  $\mathbf{A}_{kp}\mathbf{A}_p$  are the same as the eigenvalues of  $\mathbf{A}_{kp}^{1/2}\mathbf{A}_p\mathbf{A}_{kp}^{1/2}$ . The matrix  $\mathbf{A}_{kp}^{1/2}\mathbf{A}_p\mathbf{A}_{kp}^{1/2}$  is observed to be symmetric and positive semi-definite since  $\mathbf{A}_p \geq 0$ . Therefore, the eigenvalues of  $\mathbf{A}_{kp}^{1/2}\mathbf{A}_p\mathbf{A}_{kp}^{1/2}$  are real and non-negative. As a result, the non-zero eigenvalues of  $\mathbf{A}_p$  are observed to get scaled by the transformation  $\mathbf{A}_p \mapsto \mathbf{A}_{kp}^{1/2}\mathbf{A}_p\mathbf{A}_{kp}^{1/2}$ .

The mathematical model of (10) has been derived by combining active power balance laws with the droop control laws. As shown by (13), the property of  $\mathbf{A}_p$  being Laplacian is for any microgrid with any finite number of inverters connected in an arbitrary manner. Therefore, a microgrid where inverters are controlled by  $p$ - $\omega$  droop control laws will be stable for non-zero positive values of droop control gains. The matrix  $\mathbf{A}_p$  will contain a number of eigenvalues equal to zero corresponding to the number of disjoint parts of the microgrid. These eigenvalues equal to zero are an indication of the number of degrees of freedom in the model and do not play a role in the stability of the microgrid. The stability of the microgrid is decided by the non-zero eigenvalues of  $\mathbf{A}_{kp}\mathbf{A}_p$  that are positive and real. ■

The above theorem states that for the model under consideration we have stability for arbitrary positive  $p$ - $\omega$  droop control gains. The above proof of the stability of multi-inverter microgrids has certain limitations that will be discussed in detail in the next section.

#### IV. LIMITATION OF THE MATHEMATICAL MODEL

In order to examine the limitation of the mathematical model of (10), a simple microgrid will be considered to examine the manner in which its poles will change as the  $p$ - $\omega$  droop control gain changes. Fig. 4 shows a single inverter ‘‘Inverter 1’’ connected to a main ac grid. The main ac grid has a fixed frequency and is considered as the reference for measuring the phase angle of the inverter. The inverter feeds a load and is connected to the main grid through a cable with negligible resistance and inductance of  $L_{1g}$ .

Fig. 4 shows the inverter output voltage vectors in polar form. The grid voltage vector has been considered to be the reference for phase angle measurement of the inverter output voltage vector. Moreover, the grid is assumed to be stiff and frequency of the grid voltage remains constant. As a result,

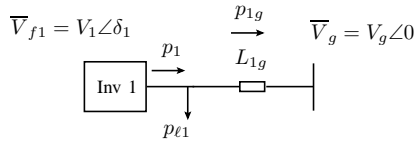


Fig. 4. Single inverter connected to a grid

the only variable in the above system is the phase angle of the inverter output voltage vector  $\delta_1$ .

The mathematical model of (10) can be written for the above simple microgrid. The matrices of (10) are scalars and are as follows:

$$\begin{aligned} \mathbf{A}_{kp} &= k_{p1} \\ \mathbf{A}_p &= \frac{3V_1 V_g}{\omega L_{1g}} \cos \delta_1 \end{aligned} \quad (20)$$

Since, the matrix equation of (10) is a single differential equation for Fig. 4, the controlled system can be represented by the block diagram of Fig. 5. In Fig. 5, the  $\frac{1}{s}$  denotes the integral operator. For the block diagram of Fig. 5, a root locus diagram can be drawn as shown in Fig. 6. The integral operator  $\frac{1}{s}$  is considered to be part of the plant along with  $\mathbf{A}_p$ . The control gain of the controlled system is the  $p$ - $\omega$  droop control gain  $\mathbf{A}_{kp}$ .

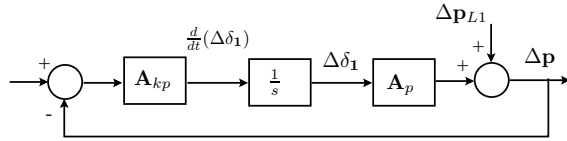
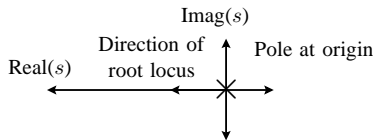

 Fig. 5. Block diagram of  $P$ - $\omega$  droop

 Fig. 6. Root locus plot with respect to  $p$ - $\omega$  droop

Fig. 6 shows the single pole at the origin due to the integral operator. The zero of the plant is at  $s = -\infty$ . Therefore, the root locus moves from the plant pole to the plant zero as  $k_{p1} \rightarrow \infty$ . From the root locus plot, it can be concluded that the controlled system will be stable for all positive values of  $k_{p1}$ . However, in practical cases, even a single inverter connected to a main grid can become unstable for large values of  $k_{p1}$  [3], [4]. Therefore, the root locus plot of Fig. 6 does not provide the stable boundary of the microgrid.

The derivation of (10) assumes that the resistance of the interconnecting cables is negligible. The assumption is relaxed at this point to examine the effect of non-zero R/X ratio of the cables on the stability results obtained above. The active power flowing between the inverter and the grid when the cable has a non-zero R/X ratio can be written along the same lines as (2):

$$p_{1g} = \frac{3V_1(V_1 - V_g \cos \delta_1)R_{1g}}{R_{1g}^2 + (\omega L_{1g})^2} + \frac{3V_1 V_g \omega L_{1g}}{R_{1g}^2 + (\omega L_{1g})^2} \sin \delta_1 \quad (21)$$

The equation can be linearized to obtain the following expression in small signal sense:

$$\Delta p_{1g} = \frac{3V_1 V_g}{R_{1g}^2 + (\omega L_{1g})^2} \left( R_{1g} \sin \delta_1 + \omega L_{1g} \cos \delta_1 \right) \Delta \delta_1 \quad (22)$$

Under the assumption that  $\sin \delta_1 \approx \delta_1$ ,  $\cos \delta_1 \approx 1$ , the closed loop equation after applying the  $p$ - $\omega$  droop control law is:

$$\begin{aligned} \frac{d}{dt}(\Delta \delta_1) &= \\ &- k_{p1} \left[ \frac{V_1 V_g}{R_{1g}^2 + (\omega L_{1g})^2} \left( R_{1g} \delta_1 + \omega L_{1g} \right) \Delta \delta_1 \right] - k_{p1} \Delta p_{\ell 1} \end{aligned} \quad (23)$$

The above controlled system equation for a microgrid with cables having non-zero R/X ratio differs from the case where R/X ratio was zero in the aspect that instability is now possible for positive values of  $k_{p1}$ . When the following condition is satisfied, the poles of the controlled system will be in the right half of the complex  $s$  plane resulting in instability:

$$\delta_1 < -\frac{\omega L_{1g}}{R_{1g}} \quad (24)$$

In order to interpret the above condition, the equilibrium state about which the system is linearized will be described. If the only load in the microgrid is connected locally at the inverter, the droop control laws will cause the load active power demand to be shared equally between the inverter and the grid. Therefore, active power will flow from the grid to the inverter and the output voltage of the inverter will lag behind the grid voltage by phase angle  $\delta_1$ . Since the grid has been assumed to be the reference for measurement of phase angle of the inverter,  $\delta_1 < 0$ . Under these circumstances, if the above condition in (24) is satisfied, the microgrid will be unstable for any value of  $p$ - $\omega$  droop control gain.

However, for a microgrid where the above condition is not satisfied, the system will be stable for all positive values of  $k_{p1}$ . This result is again contrary to the practical results, where the microgrid is known to become unstable as  $k_{p1}$  increases beyond a certain value irrespective of the resistance of the interconnecting cable. This clearly indicates that the approach of mathematical modeling used in this paper has resulted in a few critical modes being omitted.

## V. CONCLUSIONS

The stability analysis of large multi-inverter microgrids where droop control laws are implemented at each inverter is extremely important if microgrids are to be a feasible alternative towards reliable and expandable power supplies. This paper proposes a mathematical proof of stability of microgrids. In this paper, only the  $p$ - $\omega$  droop control laws have been included in the model and the voltage magnitude of the inverters have been assumed to be constant at their nominal values. The loads in the microgrids have been assumed to draw only active power. The approach undertaken in this paper has several significant contributions and limitations which will be described in detail below.

The mathematical model uses steady state power flow equations since the droop control laws require as inputs the power supplied by the inverter. Using power balance laws and power flow equations, the mathematical model developed exhibits a very elegant matrix structure. The structure of the matrix allows an analogy to the Laplacian of an undirected connected graph. Using this analogy, the poles of the microgrid have been proved to be stable for all positive values of the  $p$ - $\omega$  droop control gains. The mathematical model therefore conclusively proves the applicability of  $p$ - $\omega$  droop control laws to a multi-inverter microgrid. Furthermore, the model includes large microgrids with meshed interconnections and hence the proof is independent of topology.

The derivation of the mathematical model using steady state power flow equations assumes that the inverters are controllable power sources. As shown in the previous paper, the inverters are controlled as voltage sources and the output currents of the inverter are strongly dependent on the interconnections between inverters and the droop control laws. As a result, the dynamics of the inverter output current have been neglected in this model. A simplified model with a single inverter connected to the grid helps to illustrate this issue. The dynamics present in the controlled system are the poles at origin solely due to the integral action of the  $p$ - $\omega$  droop since frequency is varied to vary phase angle differences between inverters.

However, it has been reported in literature that large values of  $p$ - $\omega$  droop control gain result in instability of the microgrid. This is intuitive when multi-inverter microgrids are compared with conventional power systems. Large rates of change of the speed of generators will cause the generators to swing out of synchronism resulting in large power oscillations in the power system and finally a blackout. In a multi-inverter microgrid, large  $p$ - $\omega$  droop control gains cause power oscillations that increase in magnitude until the inverter protection trips the inverters to safeguard against overcurrents. While designing a multi-inverter microgrid, it is of utmost importance to ensure that the  $p$ - $\omega$  droop control gains of the inverters do not result in instability during operation. Therefore, any mathematical model for the microgrid must be able to provide the stable boundaries of the microgrid with acceptable accuracy.

The mathematical model presented in this paper shows the microgrid to be stable for all positive values of droop control gains. Therefore, the model does not provide the stable boundaries of the microgrid. The previous section considers the effect of cable R/X ratio of the simple case of a single inverter connected to a main ac grid. However, it has been found that though certain R/X ratio that violate a derived condition can result in instability, the microgrid will remain stable in other cases for all values of  $p$ - $\omega$  droop control gain. Therefore, the limitation of the approach lies in the assumption that the inverters are controllable power sources which leads to loss of important modes of the system.

#### REFERENCES

- [1] M. Chandorkar, D. Divan, and R. Adapa, "Control of parallel connected inverters in standalone ac supply systems," *IEEE Transactions on Industrial Applications*, vol. 29, no. 1, pp. 136–143, January/February 1993.
- [2] C. Godsil and G. Royle, *Algebraic Graph Theory*. Springer, 2001.
- [3] N. Pogaku, N. Prodanovic, and T. Green, "Modeling, analysis and testing of autonomous operation of an inverter-based microgrid," *IEEE Transactions on Power Electronics*, vol. 22, no. 2, pp. 613–625, March 2007.
- [4] Y. Mohamed and E. Saadany, "Adaptive decentralized droop controller to preserve power sharing stability of paralleled inverters in distributed generation microgrids," *IEEE Transactions on Power Electronics*, vol. 23, no. 6, pp. 2806–2816, November 2008.